2007

Multilayering and Ag-Doping for Properties and Performance Enhancement in YBa2Cu3O7 Films

Alexey Pan
University of Wollongong, pan@uow.edu.au

Serhiy V. Pysarenko
University of Wollongong, serhiy@uow.edu.au

D. Wexler
University of Wollongong, david_wexler@uow.edu.au

S. Rubanov
University of Melbourne

S. X. Dou
University of Wollongong, shi@uow.edu.au

Multilayering and Ag-Doping for Properties and Performance Enhancement in $YBa_2Cu_3O_7$ Films

Alexey V. Pan, Serhiy V. Pysarenko, David Wexler, Sergey Rubanov, and Shi X. Dou

***Abstract*—Much denser $YBa_2Cu_3O_7$ (YBCO) superconducting films at least 1 μm thick with smooth surfaces have been obtained after introducing (Y/Nd)BCO multilayered structures. A significant enhancement of current carrying abilities has been achieved in these pulsed laser deposited films. The critical current density (J_c) has been increased by a factor of up to three in the entire field range. The imitation of the (Y/Nd)BCO multilayered structure by using YBCO "interlayers" has also exhibited a considerable improvement in the current carrying ability. Similarities and differences between these two "multilayering" approaches, leading to the observed effects, are discussed. The presence of interfaces even without element variation is likely to be the key to the improvements observed. In order to further promote J_c enhancement, small "multilayered" additions of silver (Ag) to the films and multilayers provide various results: (i) rather strong enhancement for rather thin films and low addition levels, (ii) considerable degradation for large addition levels, and (iii) much less pronounced effect for thicker films. The enhancement of J_c is observed in zero and low magnetic fields, but has almost no effect at higher fields. All these experimental observations are discussed in terms of pinning, transparency and structural modifications introduced during the deposition of the film structures.**

I. Introduction

An enormous effort has been made to establish viable technologies for the growth of high quality $YBa_2Cu_3O_7$ (YBCO) films (and coatings). In the case of the coated conductors, the ultimate goal is to obtain YBCO coatings with high total critical current $I_c = J_cA$, where $A = w_pd_p$ is the area through which current flows (w_p and d_p are the width and thickness of the YBCO coating, respectively). The critical current density (J_c) of high quality YBCO films is very high, reaching about $0.3J_0$ of the depairing current density (J_0). This makes it very difficult for a further enhancement. A larger width is not technologically favorable. Therefore, the easiest approach would be to increase the thickness of the layers. However, superconducting films generally exhibit the following J_c dependence as a function of thickness: $J_c \propto 1/d_p$ [1]–[4].

In order to enhance the critical current density (J_c) dependence on applied magnetic field B_a and on film thickness d_p, various multilayered structures have been shown to significantly improve the current-carrying ability, microstructure and pinning in the films of relatively large thicknesses [4]–[6]. In addition, a lot of works have recently been dedicated to find effective dopants in YBCO films and coated conductors, which would lead to the $J_c(B_a)$ dependence improvement [7]–[9].

However, the nature of the critical current density enhancement and structure improvement in multilayered films is unclear. No comprehensive analysis of doped YBCO films with different thicknesses is available, nor an unambiguous explanation of the thickness dependence is provided. Moreover, no works have been carried out which would attempt to combine the positive effects of the multilayering and doping.

In this work, we investigate the multilayer deposition approach, focusing on the influence of the interfaces between the different layers on structural and electromagnetic changes. This analysis is expanding our discussion on the origin of the J_c enhancement in multilayered films. We also show the Ag-doping effect in $YBa_2Cu_3O_7$ films with different thicknesses, as well as the results of our experiments on simultaneous multilayering and Ag-doping in the YBCO films.

II. Experimental Details

High quality YBCO films, (Y/Nd)BCO multilayers and (Y/Y)BCO single element multilayers have been grown by pulsed-laser deposition with the help of KrF Excimer Laser (248 nm) on (100) $SrTiO_3$ substrates in oxygen atmosphere of 40 Pa [4]. The distance (d_{ts}) between the targets and substrates was between 3.5 to 5 cm. The deposition temperature was kept at 780°C. Both types of the multilayers [(Y/Nd)BCO and (Y/Y)BCO] have been grown with exactly the same conditions and time intervals between each layer deposition to enable a meaningful comparison and to clarify the role of the multilayering procedure in defining properties of the films. The thickness of the films considered is 1000 nm unless otherwise specified. The nominal structure of the multilayers is YBCO/(YBCO or NdBCO)/YBCO/(YBCO or NdBCO)/YBCO with the layer thicknesses ~300 nm/50 nm/300 nm/50 nm/300 nm.

To introduce silver (Ag) addition, the YBCO and Ag targets have alternatively been ablated by the laser with controlled time intervals. This approach also represents a layered deposition technique. Ag-doped YBCO films were obtained with 12.5%, 6%, 2%, 1.25% of silver. The Ag doping level in the films was estimated on the number of laser shots at the silver target. The optimal doping level was chosen for the combined deposition of multilayers and Ag-addition layers.

The samples for transmission electron microscopy (TEM) have been prepared by the dual focused ion-beam technique. The surface morphology of the films has been observed by scanning electron microscopy (SEM) at small angles (~ 10° to 20°)

Manuscript received August 29, 2006. This work is supported by the Australian Research Council, the Australian Institute of Nuclear Science and Engineering Award, and the University of Wollongong.

A. V. Pan, S. V. Pysarenko, and S. X. Dou are with the Institute for Superconducting and Electronic Materials, University of Wollongong, NSW 2522, Australia (e-mail: pan@uow.edu.au).

D. Wexler is with the School of Materials, Mechanical and Mechatronic Engineering, University of Wollongong, NSW 2522, Australia.

S. Rubanov is with the Department of Physics, University of Melbourne, 3010 Victoria, Australia.

Color versions of one or more of the figures in this paper are available online at http://ieeexplore.ieee.org.

Digital Object Identifier 10.1109/TASC.2007.899033

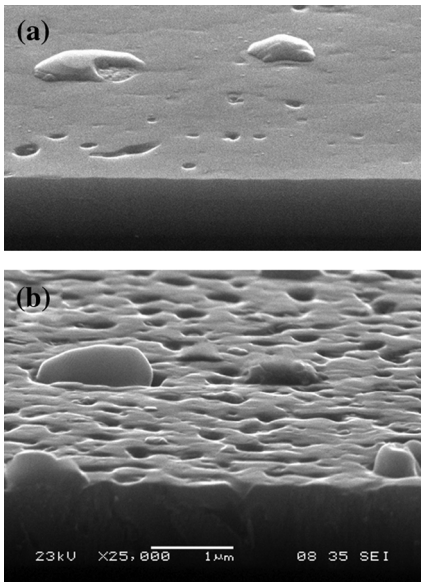

Fig. 1. SEM micrographs of the surface morphology of (a) a (Y/Nd)BCO multilayer and (b) a YBCO film with a similar thickness of about a 1 μm deposited at $d_{ts} \simeq 46$ mm.

to the plane of the surface. Electromagnetic properties of the films have been investigated by magnetization measurements over a wide applied field ($|B_a| \leq 5$ T) and temperature (5 K $\leq$ T ≤ 95 K) ranges. DC magnetic fields have been applied perpendicular to the film plane. $J_c(B_a, T)$ dependences have been obtained from the width of the magnetization loops, using the critical state model: $J_c = 2\Delta M/[w_p(1 - w_p/3l_p)]$ in A/m^2, where $\Delta M = |M^+| + |M^-|$ taken from magnetization loops measured at different temperatures, l_p is the length of the films measured.

III. Results and Discussions

A. Influence of the Multilayering

In Fig. 1, we show the surfaces of a YBCO film and a (Y/Nd)BCO multilayer for 1 μm thick samples observed by SEM. As can be seen, the multilayer (Fig. 1(a)) exhibits a much smoother surface than that in the film (Fig. 1(b)). The film is covered with holes characteristic for the spiral growth. The holes ($\sim$ 0.2 μm diameter) and corresponding structural inhomogeneity can extend throughout the entire thickness of the film. In addition, some droplets and ab-phase growth onset islands ≤ 1 μm large can be found on the surface. In contrast, the multilayers exhibit extremely smooth surfaces with only very few (smaller diameter) holes and fewer droplets.

The $J_c(B_a)$ dependences for these samples are provided in Fig. 2(a). For comparison, we also show a 0.4 μm thick YBCO film. The 0.4 μm thick film shows $J_c(0) = 3.2 \times 10^{10}$ A/m^2 in zero-field at $T = 77$ K. Strikingly, the multilayers outperform both YBCO films in the nearly entire field range.

TEM observation can provide a clue to the observed improvements, which is in line with the originally suggested scenario of the crystal lattice mismatch between YBCO and NdBCO materials [4]. The interfaces between the layers are hardly distinguishable at the crystal lattice layer scale (Fig. 3(a)). However, the layers are observed to interrupt dislocations and ab-phase

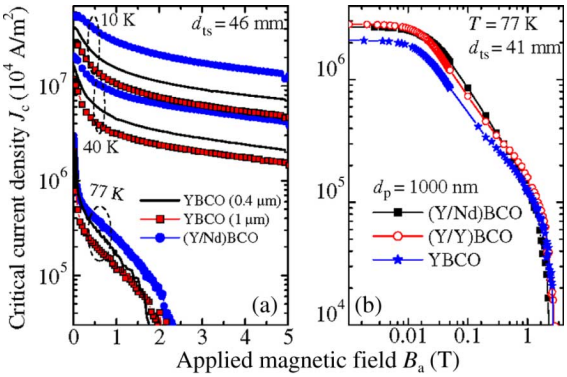

Fig. 2. (a) Critical current density as a function of applied magnetic field. YBCO monolayer films of different thicknesses and (Y/Nd)BCO multilayer deposited at $d_{ts} \simeq 46$ mm are shown. (b) $J_c(B_a)$ curves for different types of multilayers compared to YBCO film of the same thickness (1 μm) deposited at $d_{ts} \simeq 41$ mm.

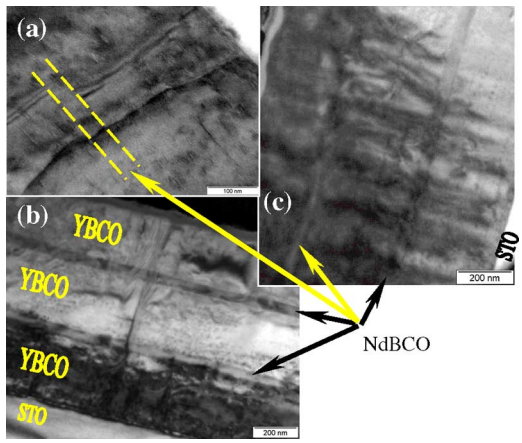

Fig. 3. TEM images of the (Y/Nd)BCO multilayer: (a) interrupted and initiated dislocations by the interface; (b) larger density of defects within the bottom YBCO layer (the darkest region); (c) additional defects (darker areas of domains transverse to the layers) produced by the interfaces. The scale bars are 100 nm for (a) and 200 nm for (b) and (c).

growth, as well as *to initiate dislocations* (Fig. 3(a), (c)). The largest density of defects is observed at the substrate/film interfaces (the darkest YBCO region between the STO substrate and the first NdBCO-layer in Fig. 3(b)). However, interfaces between the NdBCO/YBCO layers produce considerable number of additional dislocations (Fig. 3(c)). In spite of a similar mismatch between STO/YBCO and NdBCO/YBCO lattices, the number of defects initiated at the latter ones is far smaller than at the STO/YBCO interface.

The reasons proposed for the explanation of the critical current density enhancement in the multilayers with alternating layers of YBCO and NdBCO [4] or CeO_2 [5] are (i) the formation of additional mismatch dislocations at the additional interfaces [4], which are known to be effective pinning centers in YBCO films [10]; (ii) improvement of the microstructure and surface quality [4], [5] exhibiting spectacular smoothness compared to monolayer YBCO films [4]; and (iii) the increase of the filling factor due to the disappearance of holes in the films [4]. Overall, the (Y/Nd)BCO multilayers show improvements in the interface microstructures from the bottom to the top layers, as also revealed by the Rutherford backscattering [11].

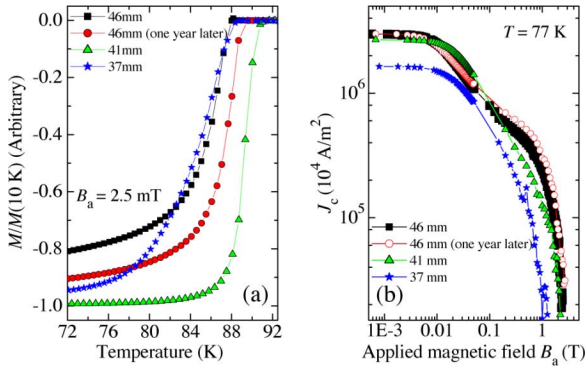

Fig. 4. (a) Normalized magnetization as a function of temperature and (b) $J_c(B_a)$ curves for (Y/Nd)BCO multilayers deposited at different d_{ts}.

The first interface between the STO substrate and the YBCO layer was found to be the roughest, whereas the surface was the smoothest. Therefore, the interchanging of the layers removes the crystal lattice stress gradually due to the local mismatch and additional dislocation formation, improving the overall structural order with fewer larger scale defects such as ab-phase growth, smaller misorientations at grain boundaries.

However, it is important to note that the surface morphology smoothness is strongly dependent on the distance between the targets and the substrate. In general it is the most sensitive parameter for production of high quality films. Not only surface morphology can be significantly roughened, but also the electromagnetic properties can be affected. As can be seen in Fig. 4, the superconducting transition T_c and $J_c(B_a)$ show considerable differences depending on the distance d_{ts}, which is identified with the precision of ± 0.5 mm. The T_c onset defined at the onset of the diamagnetism is varied from 88.8 K to 91.7 K for the (Y/Nd)BCO multilayers deposited at different d_{ts}. The best T_c transition was obtained for the film deposited at $d_{ts} \simeq 41$ mm, which assumes the best crystallinity in the film. However, this film does not show either highest J_c at low fields, or the largest pinning at high fields. It does show the longest J_c plateau at $B_a \rightarrow 0$ T. These results do not contradict to the analysis of the low field behavior provided in [12], [13]. The other parameter affecting $J_c(B_a)$ behavior at large fields but inducing no visible changes to the surface morphology and the T_c transition is the deposition temperature [4]. Growth conditions for the films are optimized to obtain same properties for every deposition, as can be seen for the multilayers deposited with the same parameters at $d_{ts} \simeq 46$ mm but with one year interval (Fig. 4).

To shed light on the influence of different interlayers and the presence of the interfaces created by "waiting", we have merely reproduced the *timing* of the (Y/Nd)BCO deposition and subsisted NdBCO interlayer by YBCO. In other words, we deposited YBCO film interrupting the deposition by the same interval which was technologically needed to grow (Y/Nd)BCO multilayer. These depositions have been done with $d_{ts} \simeq 41$ mm. The surface of the (Y/Y)BCO multilayer (not shown) is only slightly better than the surface of the YBCO films shown in Fig. 1(b) and clearly worse with larger diameter holes than the (Y/Nd)BCO multilayer. The multilayers [(Y/Y)BCO and (Y/Nd)BCO] deposited have exhibited a similar J_c enhancement compared to the YBCO monolayer film of the same thickness $\sim$ 1 μm (Fig. 2(b)). The similar

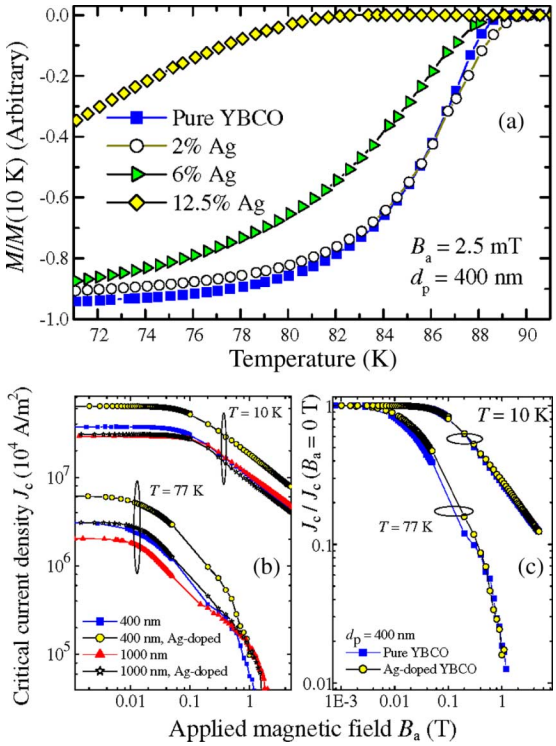

Fig. 5. (a) Normalized magnetization as a function of T; (b) $J_c(B_a)$; (c) normalized $J_c(B_a)/J_c(0)$ for the pure and Ag-doped films.

J_c enhancement which becomes pronounced upon decreasing the field indicates that the microstructures of the both multilayers improves due to the presence of the interfaces. The (Y/Nd)BCO case has been discussed above and in [4], whereas the (Y/Y)BCO interface provides microstructure related improvements which are presumably associated with the extended periods for mobile particles to find "defective" sites during the waiting time between each layer deposition. This extended mobility may result in strain release of the lattice in a similar way as NdBCO interlayers do [4], leading to J_c enhancement and some surface smoothening.

B. Silver "Multilayered" Addition

In a similar way to the multilayers, pure Ag has been added by alternating silver and the superconducting targets. It turns out that YBCO films are very sensitive to the level of the Ag addition. In Fig. 5(a), the T_c transitions for the YBCO films with added Ag are shown. The transition does not change significantly for Ag-doping level $\leq 2\%$. The onset of the critical temperature T_c for the 2% Ag doped film is $\sim$90.2 K, which is $\sim$0.6 K higher than that for the pure films from the same set. In contrast, the other Ag concentrations exhibit a lower T_c and a broader transition width.

The 2% Ag-doped film shows a quite dramatic, largest enhancement in $J_c(B_a)$ behavior (Fig. 5(b)), whereas the other doped samples experience substantial $J_c(B_a)$ degradation (not shown for clarity). $J_c(0)$ for the 2% Ag-doped 400 nm thick film outperforms the undoped film by a factor of $\sim$1.7 at 10 K and $\sim$2 at 77 K. For the thicker films with $d_p \simeq 1000$ nm, the $J_c(B_a, T)$ behavior has a very similar trend but the Ag influence is significantly smaller. At 77 K, the low field J_c for the

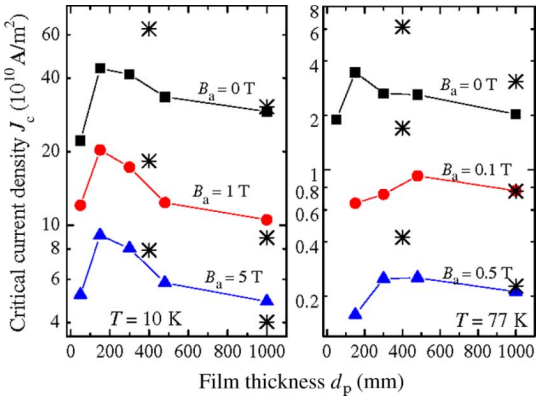

Fig. 6. $J_c(d_p)$ for the films. The asterisks mark the 2% Ag-doped films.

Ag-doped film is by a factor of ∼1.5 larger, and at $B_a \geq 0.8$ T, the $J_c(B_a)$ for pure and doped films merge. At 10 K, only marginal J_c enhancement is observed at $B_a < 0.1$ T for thicker films. Above 0.1 T, the pure sample exhibits slightly larger J_c than the Ag-doped one.

The J_c behavior of the pure YBCO films as a function of the thickness at different fields and temperatures is shown in Fig. 6. The results obtained for the 2% Ag-doped samples are indicated by the asterisks. The $J_c(d_p)$ degradation with increasing d_p in YBCO films is usually attributed to microstructural deterioration, surface roughness, porosity, ab-phase growth [1], [4].

Generally, there are two main mechanisms to increase J_c [4], [10], [13]: (i) the enhancement of the transparency for the supercurrent flow; (ii) the reinforcement of pinning. These mechanisms complement one another and also can be competing, since too many pinning sites would imply a low current transparency. In addition, they are likely to affect the different field/temperature ranges. Due to the presence of only few vortices at small fields the transparency could dominate, whereas at large fields strong pinning can be more important.

In our case, we clearly observe the more pronounced enhancement of J_c at small fields, which is in contrast to the nano-particle doping enhancing J_c at large fields only [7], [8]. This trend indicates that Ag-doping improves the transparency of the grains rather than pinning. This is consistent with previous findings of the catalyst effect of Ag in stabilizing the superconducting phase and promoting grain growth [14], [15], which can explain a slight T_c increase for our films with the optimal Ag level.

Moreover, the J_c enhancement (Figs. 5(a) and 6) is slightly larger at 77 K than at 10 K. The coherence length $\xi(T) \propto (1 - T/T_c)^{-0.5}$ is shorter at low temperatures, which means that the scattering of charge carriers is stronger at grain boundaries and structural inhomogeneities. Thus, the Ag doping can effectively rectify the reduced transparency. At higher temperatures, $\xi(T)$ is larger, so that the enhancement of the transparency by Ag would be less dramatic because the overall scattering is smaller.

If we plot the normalized $J_c(B_a)/J_c(0)$ curves (Fig. 5(b)) for the pure and 2% Ag-doped films at 10 K and 77 K, the curves for the corresponding thicknesses and temperatures almost coincide. Presumably, this implies that no change in the pining mechanism has occurred after Ag-doping, which would have changed the curvature. This also supports our scenario of the supercurrent transparency enhancement promoted by the Ag presence. Importantly, neither Ag nor Ag containing compounds has been detected in the films by x-ray diffraction (XRD) for *all doping levels* investigated. Either Ag could not be detected by XRD due to the smallness of Ag particles (< 10 nm) or Ag was oxidized and evaporated from the films. Silver oxides have quite low melting temperature (∼ 100°C to 200°C) compared to the temperature used for the deposition.

Minimal Ag influence in the thicker films and the both types of the multilayers might be due to a microstructure degradation with increasing thickness or the insufficient 2% Ag addition level for the thick films for which these experiments have been carried out.

IV. Conclusion

In conclusion, the structure related improvements introduced by the multilayered approach at the interfaces are responsible for the enhancement of current-carrying ability in relatively thick films. We have also shown that silver "doping" increases J_c at relatively low fields owing to the enhanced microstructural transparency, which is similar to the effect of Ca-doping [9] and in contrast to the J_c enhancement due to pinning reinforcement usually observed at high fields [7], [8].

References

[1] S. R. Foltyn *et al.*, "Relationship between film thickness and the critical current of $YBa_2Cu_3O_{7-\delta}$ coated conductors," *Appl. Phys. Lett.*, vol. 75, p. 3692, 1999.

[2] C. J. van der Beek *et al.*, "Strong pinning in high-temperature superconducting films," *Phys. Rev. B*, vol. 66, p. 024523, 2002.

[3] V. A. Khokhlov *et al.*, "Surface pinning as origin of high critical current in superconducting films," *Supercond. Sci. Technol.*, vol. 17, p. S520, 2004.

[4] A. V. Pan *et al.*, "Drastic improvement of surface structure and current-carrying ability in $YBa_2Cu_3O_7$ films by introducing multilayered structure," *Appl. Phys. Lett.*, vol. 88, p. 232506, 2006.

[5] Q. X. Jia *et al.*, "High-temperature superconducting thick films with enhanced supercurrent carrying capability," *Appl. Phys. Lett.*, vol. 80, p. 1601, 2002.

[6] S. R. Foltyn *et al.*, "Overcoming the barrier to 1000 A/cm width superconducting coatings," *Appl. Phys. Lett.*, vol. 87, p. 162505, 2005.

[7] J. L. Macmanus-Driscoll *et al.*, "Strongly enhanced current densities in superconducting coated conductors of $YBa_2Cu_3O_{7-x} + BaZrO_3$," *Nature Mater.*, vol. 3, p. 439, 2004.

[8] A. A. Gapud *et al.*, "Enhancement of flux pinning in $YBa_2Cu_3O_{7-\delta}$ thin films embedded with epitaxially grown Y_2O_3 nanostructures using a multi-layering process," *Supercond. Sci. Technol.*, vol. 18, p. 1502, 2005.

[9] H. Song *et al.*, "Electromagnetic, atomic structure and chemistry changes induced by Ca-doping of low-angle $YBa_2Cu_3O_{7-\delta}$ grain boundaries," *Nature Mater.*, vol. 4, p. 470, 2005.

[10] V. Pan *et al.*, "Supercurrent transport in $YBa_2Cu_3O_{7-\delta}$ epitaxial thin films in a dc magnetic field," *Phys. Rev. B*, vol. 73, p. 054508, 2006.

[11] A. V. Pan *et al.*, "Multilayered deposition and its role in the enhancement of $YBa_2Cu_3O_7$ film performance," *Physica C*, submitted for publication.

[12] A. V. Pan *et al.*, "Thermally activated depinning of individual vortices in $YBa_2Cu_3O_7$ superconducting films," *Physica C*, vol. 407, pp. 10–16, 2004.

[13] A. V. Pan and S. X. Dou, "Comparison of small-field behavior in MgB_2, low- and high-temperature superconductors," *Phys. Rev. B*, vol. 73, p. 052506, 2006.

[14] R. K. Singh *et al.*, "Improvement in the properties of high Tc films fabricated in situ by laser ablation of $YBa_2Cu_3O_7$-Ag targets," *Appl. Phys. Lett.*, vol. 60, p. 255, 1992.

[15] R. Kalyanaraman *et al.*, "The role of Ag in the pulsed laser growth of YBCO thin films," *J. Appl. Phys.*, vol. 85, p. 6636, 1999.